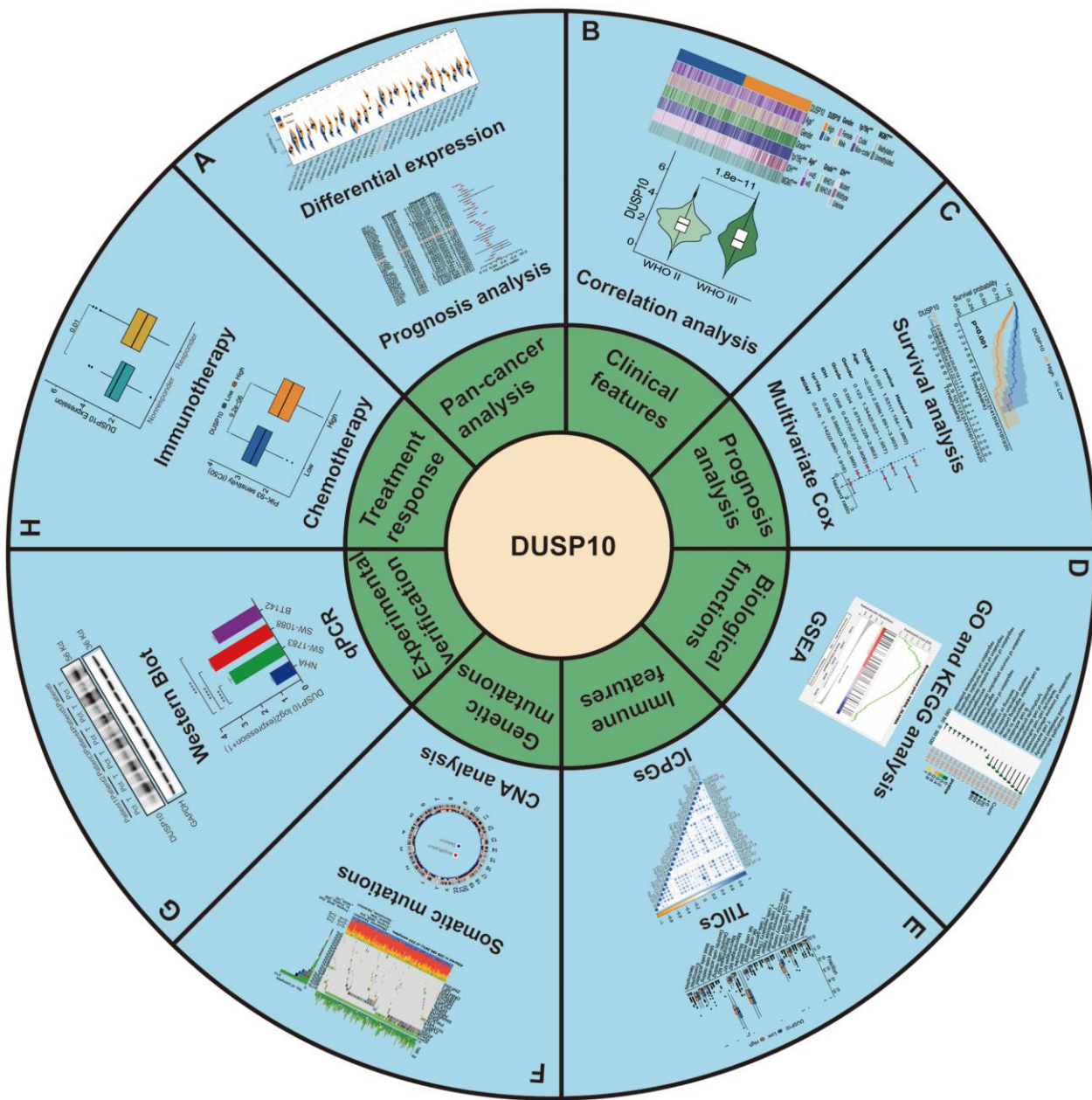
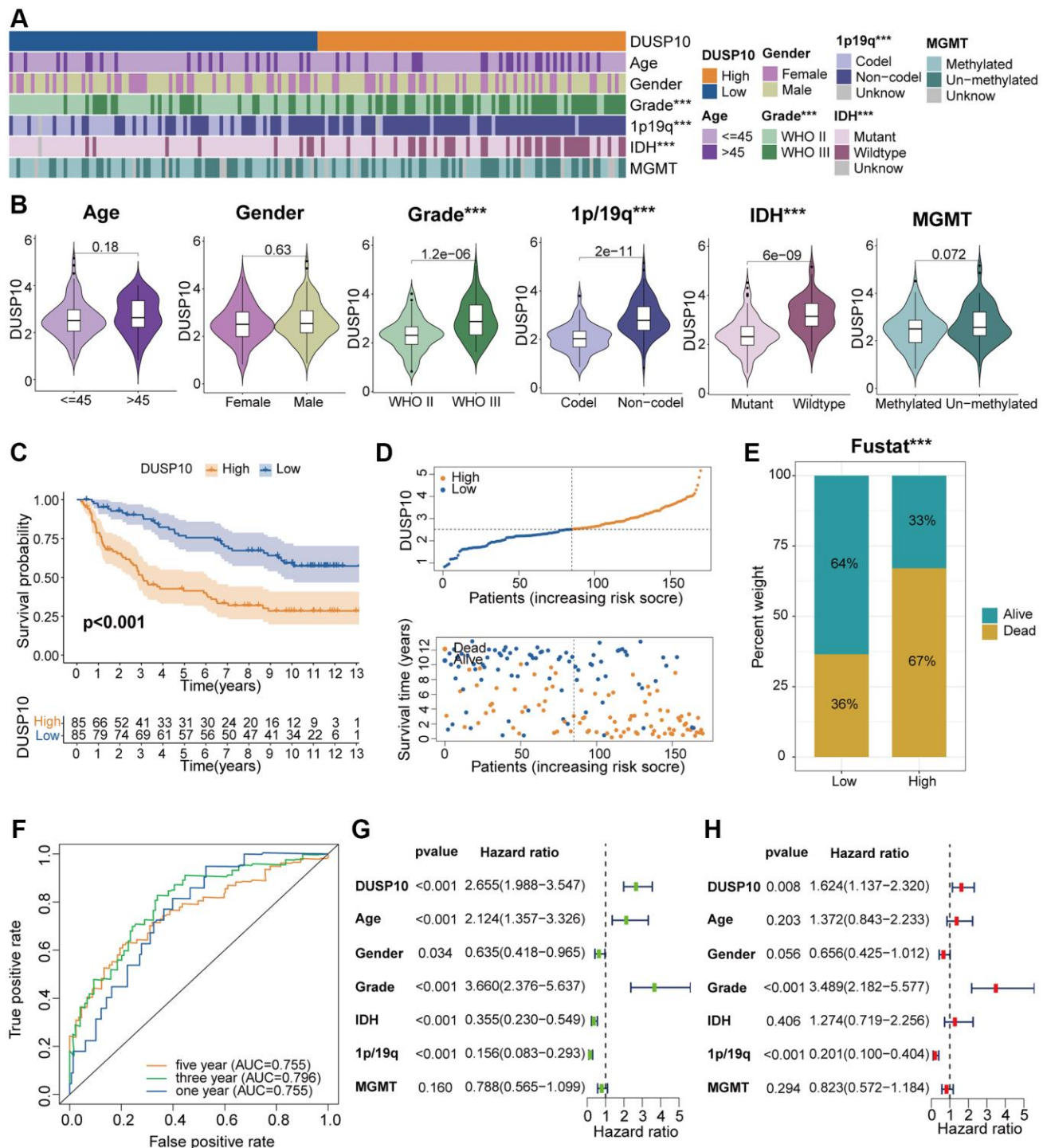


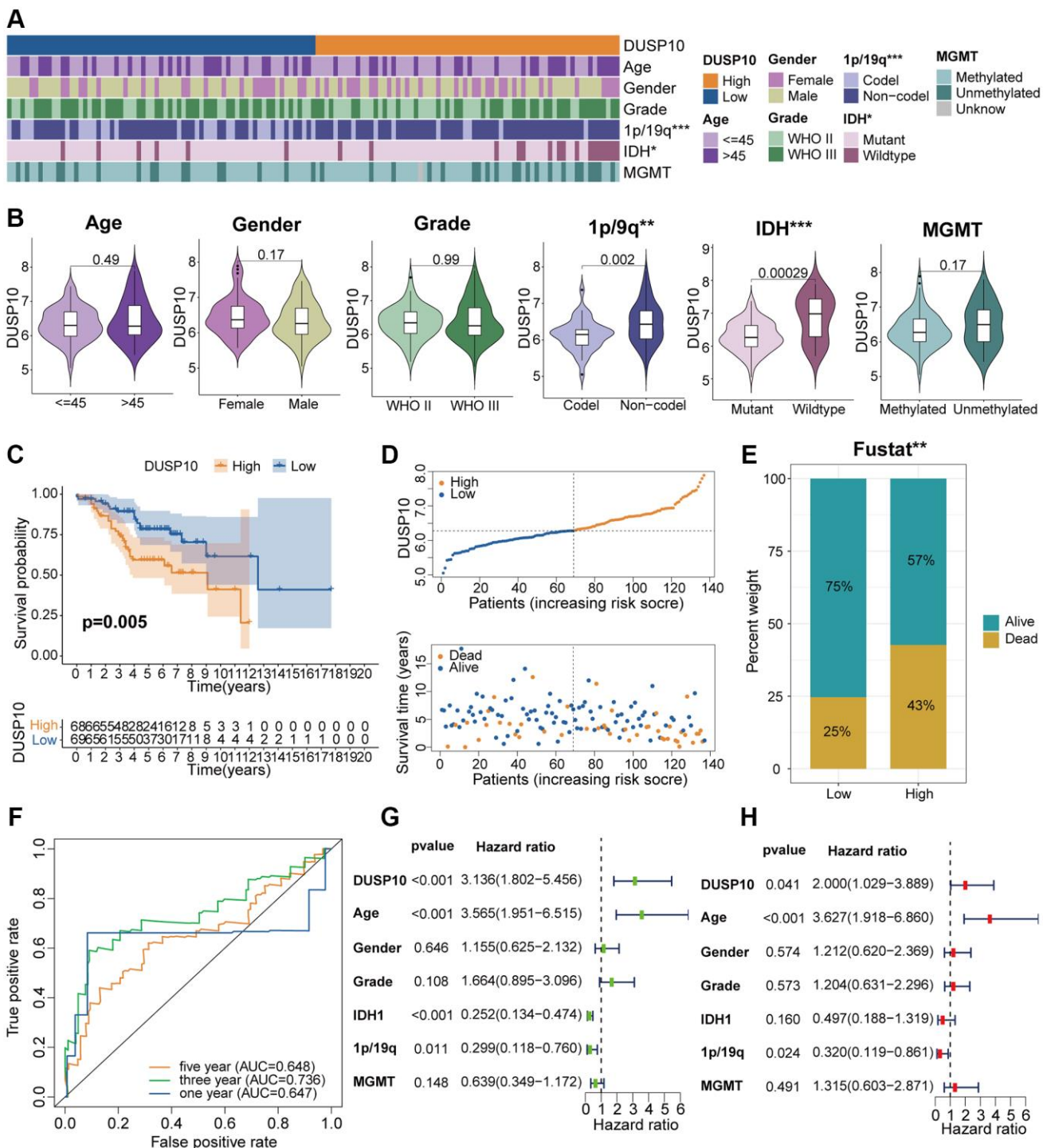
## SUPPLEMENTARY FIGURES



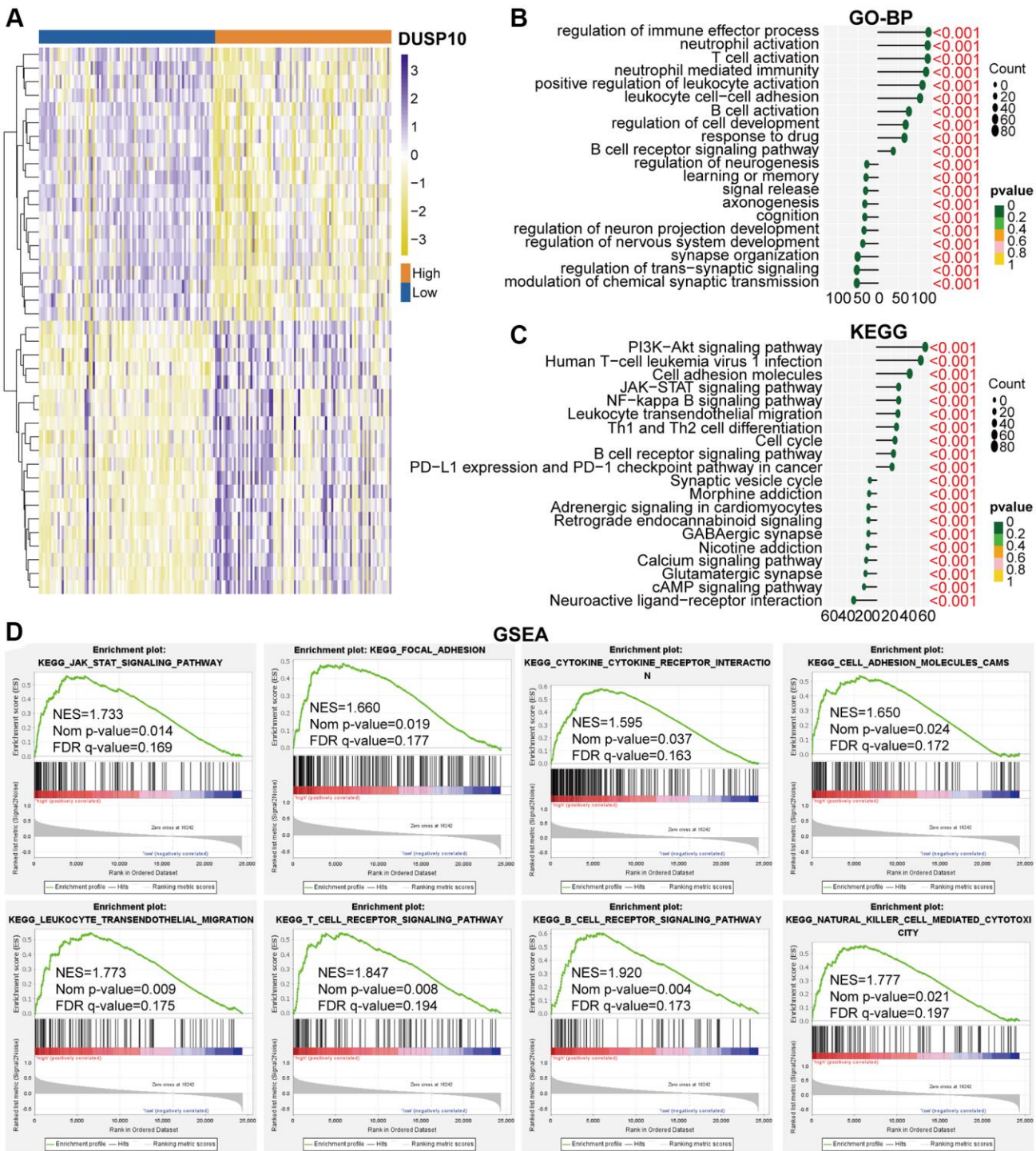
**Supplementary Figure 1. Flow diagram of overall research.** (A) Pan-cancer analysis. (B) Clinical features. (C) Prognosis analysis. (D) Biological functions. (E) Immune features. (F) Genetic mutations. (G) Experimental verification. (H) Treatment response of DUSP10 in LGG.



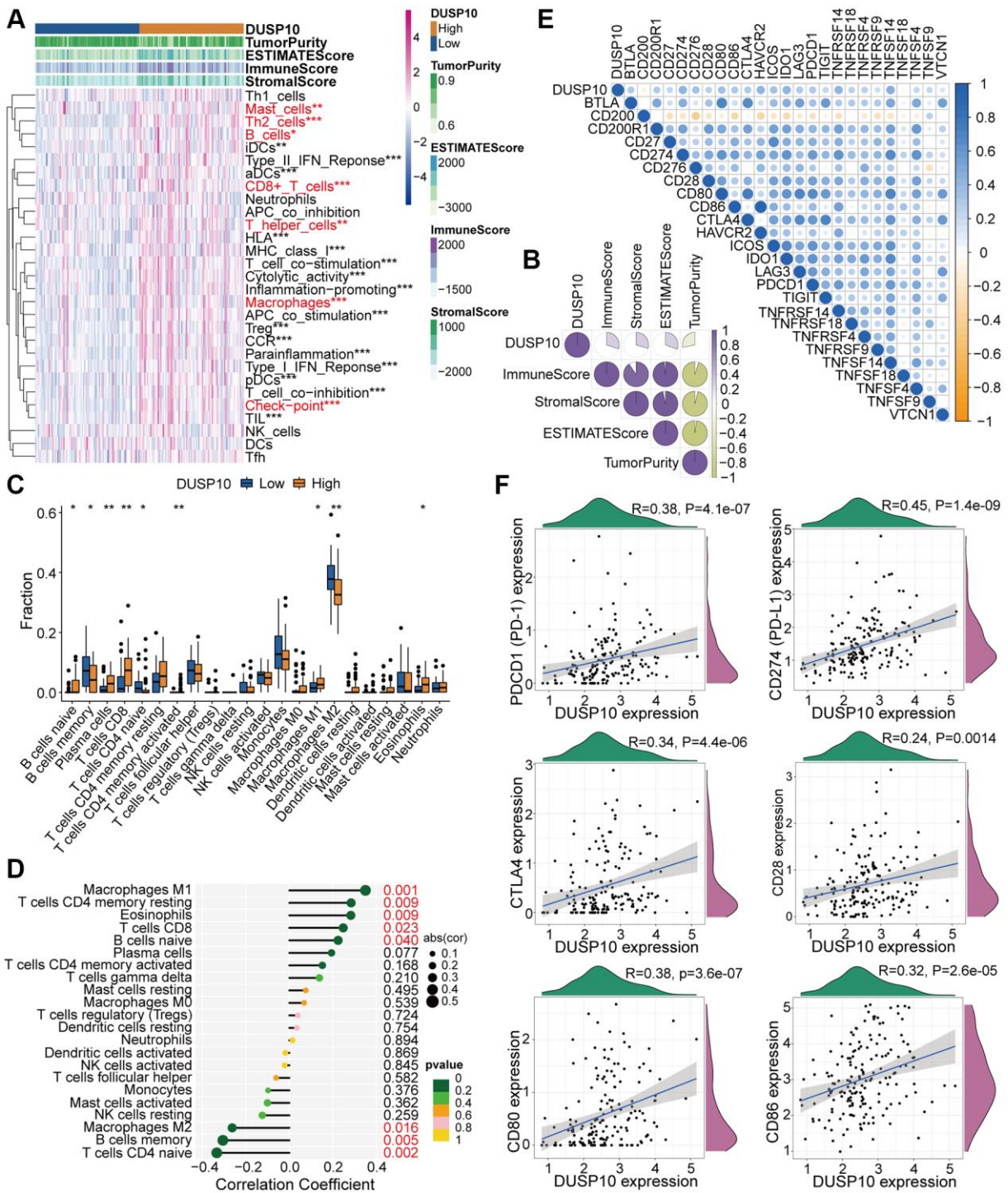
**Supplementary Figure 2. Clinical correlation analysis of DUSP10 in CGGA.** (A) Association between DUSP10 expression and clinical traits of LGG in CGGA. (B) Variance analysis of DUSP10 expression in different clinical features (including age, gender, grade, and 1p/19q, IDH, and MGMT statuses) in the CGGA dataset. (C) Prognostic analysis of high-DUSP10 and low-DUSP10 subtypes in the CGGA dataset. (D) Distribution of risk score, OS, and OS status of high-DUSP10 and low-DUSP10 subtypes in the CGGA dataset. (E) Different proportions of the living situation between the two subtypes. (F) ROC curves representing the predictive role of the risk score in CGGA. (G, H) Univariate and multivariate Cox analyses of DUSP10 expression and clinicopathological characteristics in CGGA. \*P < 0.05, \*\*P < 0.01, \*\*\*P < 0.001.



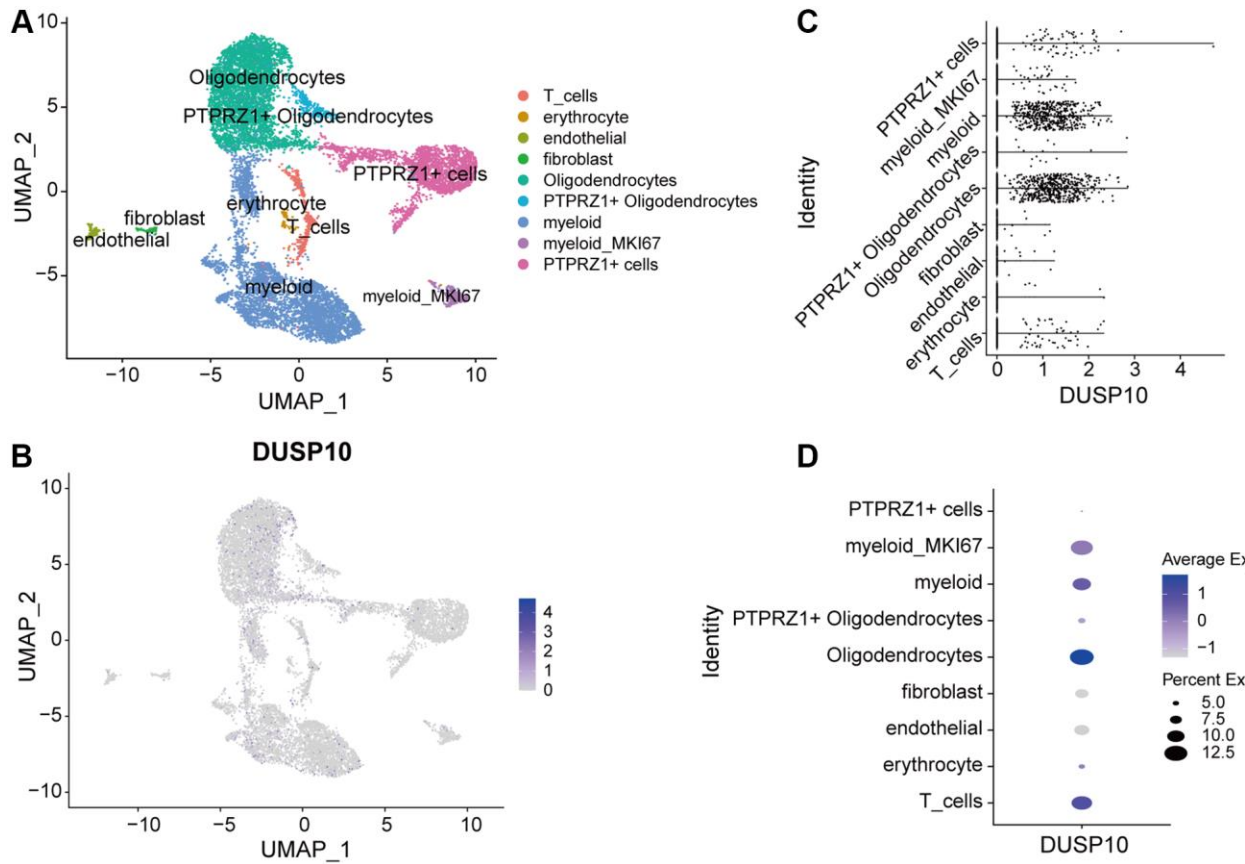
**Supplementary Figure 3. Clinical correlation analysis of DUSP10 the GSE61374 dataset.** (A) Association between DUSP10 expression and clinical traits of LGG the GSE61374 dataset. (B) Variance analysis of DUSP10 expression in different clinical features (including age, gender, grade, and 1p/19q, IDH, and MGMT statuses) in the GSE61374 dataset. (C) Prognostic analysis of high-DUSP10 and low-DUSP10 subtypes in the GSE61374 dataset. (D) Distribution of risk score, OS, and OS status of high-DUSP10 and low-DUSP10 subtypes in the GSE61374 dataset. (E) Different proportions of the living situation between the two subtypes. (F) ROC curves representing the predictive role of the risk score in GSE61374. (G, H) Univariate and multivariate Cox analyses of DUSP10 expression and clinicopathological characteristics in GSE61374. \* $P < 0.05$ , \*\* $P < 0.01$ , \*\*\* $P < 0.001$ .



**Supplementary Figure 4. Biological functions of DUSP10 in LGG in CGGA.** (A) DEGs between the low-DUSP10 and high-DUSP10 expression LGG subgroups. (B, C) The GO-BP (B) and KEGG (C) analyses for DUSP10 in LGG patients in the CGGA dataset. (D) GSEA in the CGGA dataset.



**Supplementary Figure 5. Different TME and immunological characteristics of the low- DUSP10 and high-DUSP10 subtypes in CGGA.** (A, B) Association between DUSP10 expression and 29 immune-associated signatures, ESTIMATE, immune, stromal scores, and tumor purity. (C) Comparisons of infiltration of 22 types of immune cells in the two subgroups. (D) Lollipop plots exhibited the relationship between DUSP10 expression and TIICs. (E, F) Co-expression analysis of DUSP10 and 25 ICPIGs. \* $P < 0.05$ , \*\* $P < 0.01$ , \*\*\* $P < 0.001$ .



**Supplementary Figure 6. Single-cell analysis of DUSP10 in GSE167960.** (A, B) The cell types in LGG immune microenvironment and the expression distribution of DUSP10. (C, D) Expression levels of DUSP10 in immune cells.